Noise Analysis for Multi-channel '*THz Torch*' Thermal Infrared Wireless Communications Systems

Fangjing Hu[1] and Stepan Lucyszyn[1]*

[1]Centre for Terahertz Science and Engineering, Department of Electrical and Electronic Engineering, Imperial College London, Exhibition Road, London SW7 2AZ, United Kingdom

E-mail: s.lucyszyn@imperial.ac.uk

***Abstract* — The '*THz Torch*' concept was recently introduced by the authors for providing secure wireless communications over short distances within the thermal infrared (10-100 THz). Unlike conventional systems, thermal infrared can exploit front-end thermodynamics with engineered blackbody radiation. In this paper, a noise analysis is given for this new form of wireless link, which has the potential to operate up to ~1 km in range. The mathematical modeling of a short end-to-end link is presented, which integrates thermodynamics into conventional noise power analysis. As expected from the Friis formula for noise, it is found that the noise contribution from the pyroelectric detector dominates intrinsic noise. Measured noise power is compared with calculated results. Our noise analysis can serve as an invaluable tool for the development of thermal infrared systems, accurately characterizing the noise performance of each individual channel and, thus, enables the performance of multi-channel '*THz Torch*' systems to be optimized.**

Index Terms — THz Torch, wireless communications, thermal infrared, noise analysis, blackbody radiation.

I. Introduction

Until very recently, there has been little in the way of enabling technologies within thermal infrared (*ca.* 10-100 THz) part of the frequency spectrum to support wireless communications. The authors previously demonstrated that the thermal infrared (IR) offers opportunities for developing secure communications within this largely unregulated part of the electromagnetic spectrum. The *THz Torch'* technology fundamentally exploits engineered blackbody radiation, by partitioning thermally-generated spectral noise power into pre-defined frequency channels; the energy in each channel is then independently pulsed modulated and multiplexing schemes are introduced to create a robust form of short-range secure communications in the far/mid infrared [1-6].

To assess the performance of thermodynamics-based links, accurate noise analysis is required. In this paper, we report on the noise analysis for '*THz Torch*' thermal infrared wireless communications system using engineered blackbody radiation. Here, a generic 4-channel system, having a 640 bps data rate per channel, operating with different channel transmitter bias currents over a transmission range of 1 cm is investigated. The modelled noise voltages from each of the uncorrelated channel receivers are compared with measured values.

II. System Overview

The basic architecture for a single-channel *'THz Torch'* link, without any collimating lenses, is shown in Fig. 1 [1-6]. With our setup, the transmitter consists of five incandescent light bulbs connected in series. The emitted output power is then filtered by a THz band pass filter (BPF) and the band-limited thermal noise power is modulated using ON-OFF keying (OOK). At the receiver end, the incoming energy is first filtered (by an identical THz filter as the one on the transmitter) and then detected and converted to an electrical signal by a pyroelectric (PIR) sensor. The received signal is then amplified and digitized by the post-processing circuitry, which contains a baseband low noise amplifier (LNA), baseband BPF and Schmitt trigger.

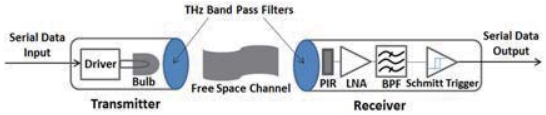

Fig. 1. Basic architecture for ultra-low cost ON-OFF keying '*THz Torch*' wireless communications link [1-6].

To determine the signal-to-noise ratio (SNR) performance of the '*THz Torch*' wireless communications system, the noise analysis for each channel receiver must be undertaken. The additive intrinsic noise for each channel can be separated out into two sources: noise from the front-end sensor and noise from the back-end electronics. The block diagram for the complete channel receiver is illustrated in Fig. 2(a). Within the channel receiver, a dual-sensor configuration is employed, where two identical PIR sensors LME-553 are used; one is a dummy sensor that is opaque to the environment, to minimize unwanted microphonic effects caused by mechanical/acoustic vibrations incident to the pyroelectric material. The output from each PIR sensor will pass through the buffering stage and is then amplified and filtered, before it is threshold detected by the Schmitt trigger (ST); the output of which is a polar NRZ signal. Intrinsic noise will be generated at each stage, and combined with noise contributions from all previous stages. The total noise of the channel receiver is evaluated at the output of the baseband BPF, as shown in Fig. 2(b). Note that without a THz BPF the intrinsic noise performance would not be channel specific. Also, noise

contribution from the ST is not included here as signal and noise power are measured at the output of the baseband BPFs.

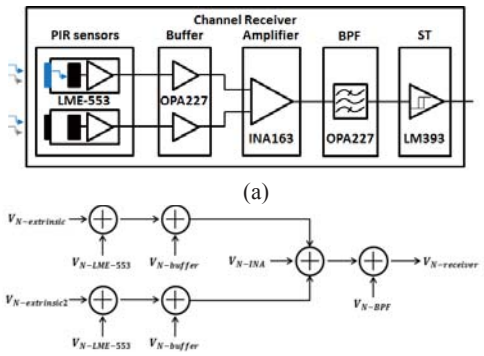

Fig. 2. Complete channel receiver: (a) detailed block diagram; and (b) noise contributions.

III. Noise Analysis

A. Pyroelectric Infrared Sensor Noise Sources

The pyroelectric sensor transduces not only the useful incident noise power but also ambient background noise. With our current mode TIA-based PIR sensor LME-553, there are a number of intrinsic noise sources, which include: temperature noise V_{NT}, due to temperature fluctuation; dielectric noise V_{ND}, due to the dielectric loss associated with the pyroelectric material; noise from the input resistance V_{NR}; noise from the large feedback resistor V_{NFB}; current noise from the TIA's operational amplifier (op-amp) V_{NI}; and voltage noise from the op-amp V_{NU}. Fig. 3 shows the calculated voltage-noise spectral densities for each individual noise source for the LME-553 PIR detector. Note that for the parameters not specified in LME-553 datasheets, typical values for similar $LiTaO_3$ type PIR detectors have been given.

From these calculations, it can be seen that V_{NFB} dominates at lower modulation frequencies, due to the large feedback resistor. At modulation frequencies above 200 Hz, V_{NU} dominates, because of the large equivalent input voltage-noise spectral density at the input of the op-amp. It is also shown that V_{ND} surpasses all but V_{NU} above 200 Hz. Noise from temperature fluctuation, input resistance and op-amp current noise, are less significant.

The overall voltage-noise spectral density VN-LME-553 can be calculated from the summation of each individual noise source contribution:

$$V_{N-LME-553} = \sqrt{V_{NT}^2 + V_{ND}^2 + V_{NR}^2 + V_{NFB}^2 + V_{NI}^2 + V_{NU}^2}\ [\mathrm{V}/\sqrt{\mathrm{Hz}}] \quad (1)$$

Fig. 4 shows the calculated overall voltage-noise spectral density and the measured results given by the LME-553 datasheet [7]. It can be seen that there is excellent agreement at low frequencies; discrepancy above this frequency is mainly due to not having exact values for all parameters.

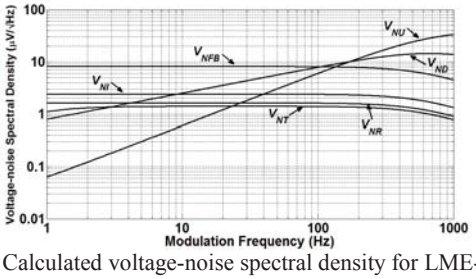

Fig. 3. Calculated voltage-noise spectral density for LME-553.

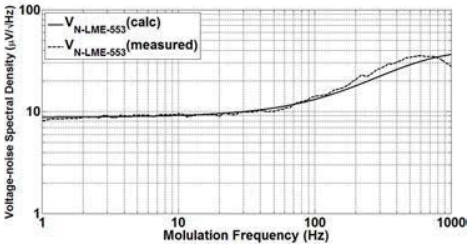

Fig. 4. Calculated and measured [7] total voltage-noise spectral density for LME-553.

By integrating over the modulation bandwidth, assuming a 1 Ω reference load resistance, the total noise power for a single LME-553 PIR sensor can be calculated as

$$N_{LME-553} = \int_{f_{m1}}^{f_{m2}} V_{N-LME-553}^2\, df_m [\mathrm{W}] \quad (2)$$

where $f_{m1} = 1$ Hz and $f_{m2} = 1$ kHz are the lower and upper modulation frequencies. The noise power is calculated to be 0.84 μW. Note that there are a number of additional sources of unwanted signals at the PIR sensor (mostly associated with the environment), such as atmospheric noise, fluctuations in ambient temperature, stray electromagnetic interference and microphonics. These extrinsic effects can only be modelled once specific ambient deployment conditions are known and thus are not considered further here.

B. Back-end Electronics Noise Sources

The back-end electronics is used to further amplify the output signal from the PIR sensor and also filter-out unwanted noise from the PIR sensor. With our particular circuit, two identical PIR sensors were used for noise reduction. The output from each detector passes through a unity gain buffer amplifier. The small-signal output voltage will be amplified by a common low-noise instrumentation amplifier (INA), having a designed voltage gain of 100. The signal from the output of the INA is then filtered by a 4th-order Sallen-Key Butterworth baseband BPF, having a designed center frequency of 320 Hz (corresponding to the modulation frequency of 320 Hz). Therefore, the noise from the back-end electronics include: voltage and current noise from the external op-amps (OPA227) used in buffer and filter stages; voltage and current noise from the instrumentation amplifier (INA163); and noise from all the resistors. It should be noted that burst and avalanche noise sources associated with op-amps are too small to be considered further [8].

Fig. 5 shows the simulated voltage-noise spectral density for a single LME-553 PIR detector ($V_{N-LME-553-output}$), back-end noise sources (V_{N-BE}) of the channel receiver and the total noise for the complete channel receiver ($V_{N-receiver}$). As expected, the former predominantly dominates the channel receiver; while the latter can be ignored at all but very low modulation frequency (where flicker noise dominates).

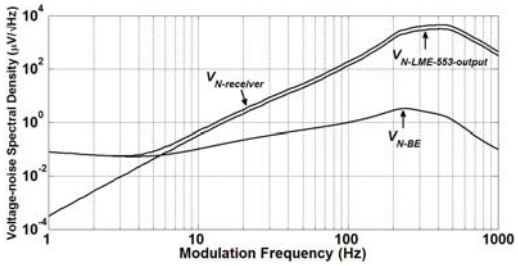

Fig. 5. Voltage-noise spectral density for a single LME-553 and back-end noise source contributions to the channel receiver.

C. Channel Receiver Noise Measurements

The noise performance for each channel receiver is measured directly using a PicoScope 2205 MSO digital oscilloscope. A noise floor at 65 μV_{RMS} was first recorded by short-circuiting the high-impedance input of the oscilloscope. The duration of the measurements was 5 minutes for each channel. Since RMS values of noise voltage can be measured directly, the corresponding total noise power can be calculated, given in Table I, where *Opaque* and *Filter* denote the PIR detector having either a blocked aperture or filled with its assigned channel THz BPF, respectively.

TABLE I
PIR DETECTOR AND RECEIVER NOISE POWER

Channel	$N_{LME-553}$ (μW)			$N_{receiver}$ (mW)	
	Calculated	Measured		Calculated	Measured
		Opaque	Filter		
A	0.84	2.50	2.34	6.52	6.89
B	0.84	2.22	2.25	6.52	6.45
C	0.84	2.40	2.19	6.52	5.12
D	0.84	1.96	1.74	6.52	4.16

When compared with the calculated value of $N_{LME-553}$ = 0.84 μW, the measured values are 2 to 3 times higher. This discrepancy is due to two main practical reasons: first, the calculated values were obtained by integrating over a modulation bandwidth from 1 Hz to 1 kHz, while the noise coupled into the PIR sensor is much wider. Second, in practice, the PIR sensor is exposed to background ambient conditions; extrinsic noise sources *in situ* are coupled into the detector, but are not included in the simulations. It should be noted that the calculations are based on values from the data sheet, which does not give information on measurement conditions.

When considering the output noise power from the complete channel receiver, there is generally good agreement; for Channels C and D their measured values are smaller than the predicted value of $N_{receiver} = 6.52$ mW. This is because there is no THz BPF applied in the simulations (i.e. values are not channel dependent). When the channel THz BPFs are included, more of the extrinsic ambient background noise is filtered out as the channel frequency increases, leading to lower measured values when compared to those calculated. Also, the noise sources from the two PIR detectors are considered to be totally uncorrelated in the calculation, which may not be the case in practice.

IV. CONCLUSION

The noise analysis for the '*THz Torch*' thermal infrared banded-noise wireless link has been investigated. The noise contributions from both PIR detectors and back-end electronics have been considered. This analysis can create a useful insight into the practical operation at both component and systems levels. With further refinement, it will prove to be an invaluable tool for engineering optimal performances with single and multi-channel systems. For example, signal levels can be adaptively controlled and equalized; simply by changing the source bias currents for each channel, thus, balancing out the performance (e.g., having the same minimum output SNR across the channels) of the complete multi-channel system. This can further increase data rates, while also improving the resilience of the system to interception and jamming at the physical layer.

ACKNOWLEDGEMENT

This work was partially supported by the China Scholarship Council (CSC).

REFERENCES

[1] S. Lucyszyn, H. Lu and F. Hu, "Ultra-low cost THz short-range wireless link", in *IEEE Int. Micro. Workshop Series on Milli. Wave Integ. Techn.*, Sitges, Spain, pp. 49-52, Sep. 2011.

[2] F. Hu and S. Lucyszyn, "Ultra-low cost ubiquitous THz security systems", in *Proc. of the 25th Asia-Pacific Micro. Conf. (APMC2011)*, Melbourne, Australia, pp. 60-62, Dec. 2011.

[3] F. Hu and S. Lucyszyn, "Improved 'THz torch' technology for short-range wireless data transfer", in *IEEE Int. Wireless Symp. (IWS2013)*, Beijing, China, Apr. 2013.

[4] F. Hu and S. Lucyszyn, "Emerging thermal infrared 'THz Torch' technology for low-cost security and defence applications", Chapter 13, pp. 239-275, "*THz and Security Applications*", NATO Science for Peace and Security Series B, C. Corsi and F. Sizov (Eds), Springer Netherlands, Apr. 2014.

[5] X. Liang, F. Hu, Y. Yan and S. Lucyszyn, "Secure thermal infrared communications using engineered blackbody radiation", *Sci. Rep.*, Nature Publishing Group, vol. 4, Jun. 2014.

[6] X. Liang, F. Hu, Y. Yan and S. Lucyszyn, "Link budget analysis for secure thermal infrared communications using engineered blackbody radiation", *XXXI General Assembly and Sci. Symp. of the Int. Union of Radio Science*, Beijing, China, Aug. 2014.

[7] InfraTec, "LME-553 datasheet", 2012. [Online]. Available: http://www.infratec-infrared.com/Data/LME-553.pdf

[8] Texas Instruments, "Application report SLVA043B: noise analysis in operational amplifier circuits", 2007. [Online]. Available: http://www.ti.com/lit/an/slva043b/slva043b.pdf